Science World Journal Vol. 21(No 1) 2026 https://dx.doi.org/10.4314/swj.v21i1.56
www.scienceworldjournal.org
ISSN: 1597-6343 (Online), ISSN: 2756-391X (Print)
Published by Faculty of Science, Kaduna State University

Full Length Research Article

VIBRATIONAL MODES AND IR-ABSORPTION OF SOME ACENE-BASED MOLECULAR JUNCTIONS. A DFT APPROACH AS IMPLEMENTED IN FHI-AIMS CODE

*[1]Kassim L. Ibrahim, [2]G. Babaji, [2]G.S.M. Galadanci, [2]A.S. Gidado, [1]Y. Shehu

[1]Physics Department, Aliko Dangote University of Science and Technology, Wudil, Kano, Nigeria
[2]Department of Physics, Bayero University, Kano, Nigeria.

*Corresponding Author Email Address: ikassim27@gmail.com Orcid ID: 0009-0005-8803-5500

ABSTRACT
There has been a recent surge in interest in studying molecular junctions made up of small acenes, such as anthracene, tetracene, and pentacene. Apart from the known transport properties exhibited by molecular junctions, there are other areas of interest, such as photothermal applications. Materials that can absorb and convert infrared radiation into heat energy can be applied in these areas. Density functional theory (DFT) calculations were used to evaluate the IR absorption of some acene-based MJs, as well as their rotational and translational energies. The results obtained were then compared with previously reported work on acene molecules. It is found that the total energy and maximum forces of these MJs converged, and the structures relaxed to the minimum possible energy. For the vibrational analysis, the maximum IR-absorption of 4.92 $D^2/Å^2$ was observed at a frequency of 688.52 cm^{-1} for an anthracene MJ. It is 2.17 Debye square per Armstrong square (D2/Å2) at a frequency of 3411.82 cm-1 and 2.93 D2/Å2 at a frequency of 648.71 cm-1 for tetracene and pentacene MJs, respectively. IR absorption at different frequencies enables one to choose the desired materials for a specific task at a given frequency.

Keywords: IR-absorption, Vibration, Convergence, Acene, DFT

INTRODUCTION

Organic materials are compounds that consist of the carbon-hydrogen bond. The electronic properties of these materials can change upon the addition of chemical groups, and their structural characteristics can also be altered. Also, they have mechanical flexibility, and their manufacturing methods are simple, inexpensive, and accessible. Almost all organic materials are dielectric and have long been used as electrical insulators (Aviram & Ratner, 1974; Heath & Ratner, 2003; Sadeghi *et al.,* 2014). Also, these molecules share π-bonds; electron hopping between π-orbitals leads to semiconducting behavior (Kaneko *et al.,* 2013). Therefore, these materials are highly regarded in electronic and spintronic applications (Aadhityan, Preferencial, and John, 2020; Lucas *et al.,* 2021; Li *et al.,* 2021). There is hope that organic semiconductors can replace the traditional silicon semiconductors. Previous studies have shown that molecular junctions (MJs) are primarily investigated for their applications in charge transport in molecular electronics (Ibrahim *et al.,* 2022). However, there are other areas where these materials (MJs) can be applied, such as dye-sensitized solar cells (DSSC) (Babaji, 2015), heat-retaining materials, heat-transfer systems (Yunus & Afshin, 2015), or solar thermal collectors for high IR-absorbing materials.

High IR absorption implies that the material can efficiently absorb and convert infrared radiation into heat. This absorption can result from the material's molecular structure and composition. The absorbed energy raises the material's temperature, making it a suitable candidate for thermally related applications. Materials with high IR absorption can absorb infrared radiation and convert it into heat for various applications, such as energy generation.
In this work, DFT calculations were used to evaluate and analyze the vibrational frequencies and IR absorption properties of anthracene-, tetracene-, and pentacene-based MJs. Variations in rotational and translational energy with temperature are also observed herein.

A basis set is a finite collection of atomic-like functions used to form the molecular orbital through a linear combination of atomic orbitals (LCAO). There are various options for basis sets, including Slater-type orbitals (STOs) and Gaussian-type Orbitals (GTOs). Wave functions, also referred to as stationary states or energy eigenstates, are essential in molecular modeling (Engel, 2002). They can be described by the time-independent Schrödinger equation (1), which is a fundamental equation in quantum mechanics that governs the behavior of electrons in molecules (Joita *et al.,* 2021). Understanding and solving this equation is crucial for determining the most accurate molecular structures and energetics (Kohn & Sham, 1965).

$$H\psi = E\psi, \quad (1)$$

where ψ is the state vector of the quantum system, E is the energy, and H is the Hamiltonian
operator.
In the time-independent Schrödinger equation (Schrödinger, 1926), the operation may produce specific values for the energy called energy eigenvalues. In addition to its role in determining system energies, the Hamiltonian operator generates the time evolution of the wavefunction in the form:

$$H\psi = j\hbar\frac{\partial}{\partial t}, \quad (2)$$

where the j constant is the imaginary unit, $\hbar$ is the reduced Planck constant, and t is time.
The Schrödinger equation provides a method for calculating the wave function of a system and its time evolution. The equation is a wave equation expressed in terms of the wave function, which analytically and precisely predicts the probability of events or outcomes. The spatial part needs to be solved for in time-independent problems, because the time-dependent phase factor is always the same.
The calculation of the free energy of vibration and rotation (rigid-rotor approximation) can be requested using this keyword. They

Science World Journal Vol. 21(No 1) 2026 https://dx.doi.org/10.4314/swj.v21i1.56
www.scienceworldjournal.org
ISSN: 1597-6343 (Online), ISSN: 2756-391X (Print)
Published by Faculty of Science, Kaduna State University

are calculated between the temperatures Tstart (K) and Tend (K) with a total of Tpoints steps. The implemented equations (3) and (4) are written as:

$$F_{vib}(T) = \sum_{I}^{3N-6}\left[\frac{\hbar\omega_i}{2} + k_B T ln\left(1 - \frac{-\hbar\omega_i}{e^{k_B T}}\right)\right] \quad (3)$$

with N being the number of atoms in the molecule and ω_i depicting the vibrational frequencies.

$$F_{rot}(T) = -\frac{3}{2}k_B T ln\left[\frac{2k_B T}{\hbar^2}(I_A I_B I_C)^{1/3}\pi^{1/3}\right] \quad (4)$$

where I_A, I_B, and I_C depict the moments of inertia of the molecule. The free energy of translation is calculated within the given temperature range, with vibrational free energy, and over the pressure range p-start (Pa) to to$p$end (Pa) with p-points steps. The equation reads:

$$F_{trans} = -k_B T\left[ln\frac{k_B T}{p} + 1 + ln\left(\frac{mk_B T}{2\pi\hbar^2}\right)^{3/2}\right] \quad (5)$$

with *p* denoting the partial pressure.

MATERIALS AND METHODS

The DFT total-energy and structure-relaxation calculations for these structures were performed. The geometry of these structures is relaxed towards their minimum energy using really tight settings in *third_tier*. These settings improved the energy relaxation from -0.25 meV to -0.12 meV. For relaxing the geometry, a keyword "relax_geometry" specifies a geometry relaxation using the BFGS algorithm, together with a standard SCF convergence criterion for the forces (sc_accuracy_forces) of 10^{-4} eV/Å, and energies (sc_accuracy_forces) of 10^{-4} eV, in the final geometry. The control in the directory also includes other general keywords concerning the technicalities of obtaining self-consistency, such as occupation_type; Gaussian 0.01, a mixing parameter; charge_mix_param; 0.5 for the mixer (nonlinear optimization of the s.c.f. cycle); and convergence criteria for the s.c.f. cycle.
Reinitialization, s.c.f., and geometry optimization information are repeated for each successive geometry step until the optimum geometry is found within the force tolerance specified by relax_geometry. These involve the following steps;

1.1 Structure modeling: The modeling of MJs was done using the computer code Jmol, version 14.6.4. The geometry of these structures was relaxed towards their minimum energy. The relaxation criteria used really tight settings (tier 3), down to BFGS 10-2 eV/Å. To relax the geometry, the keyword "relax_geometry" specifies a geometry relaxation using the BFGS algorithm. Thus, no force component for any atom of the relaxed structure should exceed 10^{-2} eV/Å. The extended structures of molecular junctions are formed using Au-clusters as source and drain electrodes. DFT electronic structure calculations were performed using the FHI-aims program (Blum et al., 2009), with the Perdew-Burke-Ernzerhof (PBE) exchange-correlation functional to ensure accuracy and reliability.

1.2 Geometry optimization: The geometry of the acene MJs was optimized using DFT. This involves finding the lowest-energy configuration of the structure by iteratively adjusting the atomic positions until the forces on each atom are minimized. This step ensures that the molecules are in their most stable geometry.

1.3 Vibrational Frequency Calculation: After obtaining the optimized geometry, the vibrational modes of the MJs were determined. Vibrations for non-periodic (cluster) structures were computed in FHI-aims using script-based finite-difference approaches. Each tool first does all necessary DFT calculations and then calls a routine to set up and diagonalize the Hessian matrices. The relevant Perl scripts and source code for this step for the entire finite-difference calculation are included with FHI-aims. With the same Makefile settings as for the main program, the 'make vibrations. scalapack.mpi' script was invoked. The frequencies obtained from this calculation provide information about the vibrational modes and their associated energies.

1.4 Thermodynamic Analysis: The obtained vibrational frequencies can be used to calculate the vibrational partition function, which is required to determine the free energy of vibration. This is done using statistical-mechanical methods, such as the harmonic oscillator approximation, or more advanced techniques like the quasi-harmonic approximation.

1.5 Rotational Analysis: The free energy of rotation can be estimated by considering the rotational partition function, which depends on the molecular moments of inertia. The moments of inertia are calculated by diagonalizing the inertia tensor, which is derived from the atoms' masses and positions in the molecule. The rotational partition function can then be obtained using standard statistical mechanical methods.

1.6

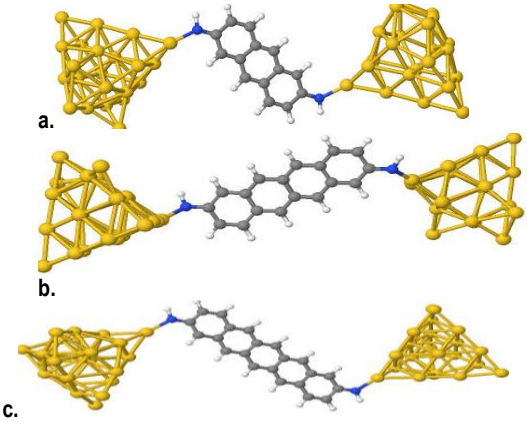

Figure 1: Optimized structures of anthracene (a), tetracene (b), and pentacene (c) MJs

RESULTS AND DISCUSSION

Results obtained are presented in this section. Instead of using frequencies to show the observed radiation, wavenumbers ($\bar{\upsilon}$, in units of cm^{-1}) are used as a conventional computational way. The wavenumber is the reciprocal of wavelength. As for the IR-absorption, the radiation was computed in Debye squared per Angstrom squared ($D^2/Å^2$), such that $1D = 3.3356 \times 10^{-20}\ C Å$.

Structure Optimization

The geometry of MJs generated from the Jmol modeling code was cleaned and optimized. The results obtained from the optimization of these built structures were presented in Tables 1, 2, and 3.

Science World Journal Vol. 21(No 1) 2026 https://dx.doi.org/10.4314/swj.v21i1.56
www.scienceworldjournal.org
ISSN: 1597-6343 (Online), ISSN: 2756-391X (Print)
Published by Faculty of Science, Kaduna State University

Table 1: Results from optimizing anthracene MJ

S.No.	Quantity	Amount
1	Number of Self_Consistency cycles	1351
2	Number of relaxation steps	65
3	Total time (wall_clock)	168088.656 s
4	Total number of basis functions	2738
5	Species_default	Third tier (*really_tight)*
6	Total energy	-23586339.2307283 eV

Table 2: Results from optimizing tetracene MJ

S.No.	Quantity	Amount
1	Number of Self_Consistency cycles	1721
2	Number of relaxation steps	99
3	Total time (wall_clock)	209716.030 s
4	Total number of basis functions	2804
5	Species_default	Third tier (*really_tight)*
6	Total energy	-23590518.5443106 eV

Table 3: Results from optimizing pentacene MJ

S.No.	Quantity	Amount
1	Number of Self_Consistency cycles	3755
2	Number of relaxation steps	135
3	Total time (wall_clock)	414114.355 s
4	Total number of basis functions	2738
5	Species_default	Third tier (*really_tight)*
6	Total energy	-23594698.1453751 eV

As shown in Tables 1, 2, and 3, the number of self-consistency cycles varies with structure size. In the process of optimizing these structures, anthracene MJ undergoes 1351 cycles with 65 relaxation steps, while tetracene and pentacene MJs undergo 1721 and 3755 cycles, with relaxation steps of 99 and 135, respectively. The total time taken to relax these structures and the minimum energy reached also depend on molecular size. These results imply that the size of the materials in question increases the computational costs. This claim is supported by Donatella and Lorentz *(2021) and Babaji* (2015).

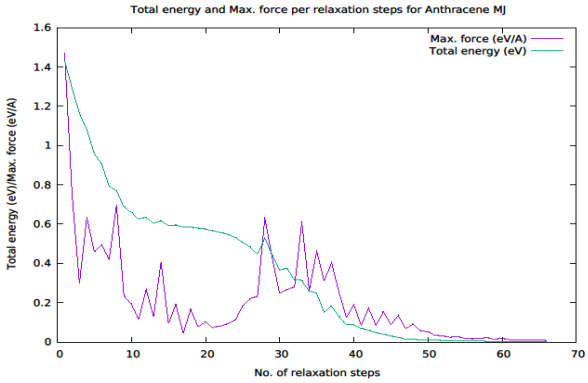

Figure 2: Energy and force convergence for anthracene-based molecular junction

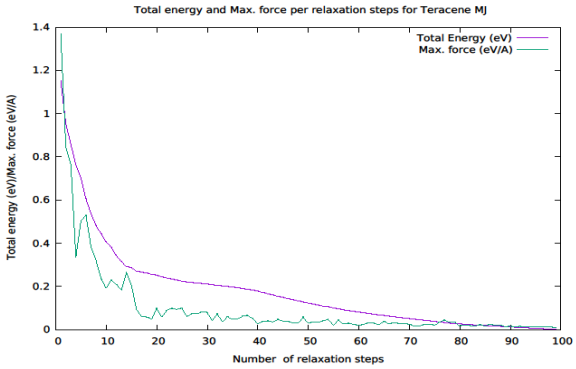

Figure 3: Energy and force convergence for tetracene-based molecular junction

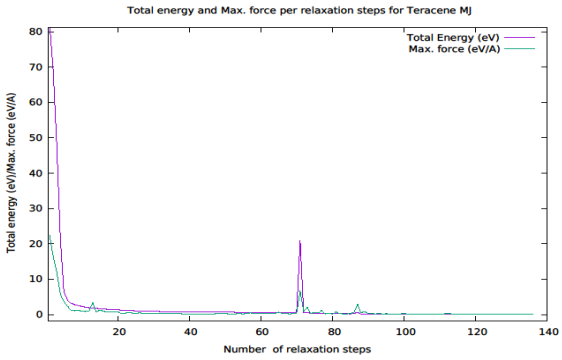

Figure 4: Energy and force convergence for pentacene-based molecular junction

The total energy convergence and force convergence are presented in Figures 2, 3, and 4. The total energies are converged. For an anthracene MJ, the energy converged from -23586337.7977226 eV to -23586339.2307283 eV. For the tetracene MJ, energy is converged from -23590517.392064 eV to -23590518.5443106 eV. Moreover, for the pentacene MJ, the energy converged from -23594615.7926751 eV to -23594698.1453751 eV. The forces also converge, following a similar pattern with their respective energies. For an anthracene MJ, the maximum force converged from 1.4659 eV/Å to 0.00708669 eV/Å. For the tetracene MJ, the maximum force

Science World Journal Vol. 21(No 1) 2026 https://dx.doi.org/10.4314/swj.v21i1.56
www.scienceworldjournal.org
ISSN: 1597-6343 (Online), ISSN: 2756-391X (Print)
Published by Faculty of Science, Kaduna State University

converged from 2.07131 eV/Å to 0.0098096 eV/Å. Also, for the pentacene MJ, the maximum force converged from 22.2951 eV/Å to 0.00789671 eV/Å.

Vibrational Analysis

Results for vibrational analysis are presented as frequency (wavenumber), free energy, and IR absorption in Figures 5, 6, and 7, respectively.

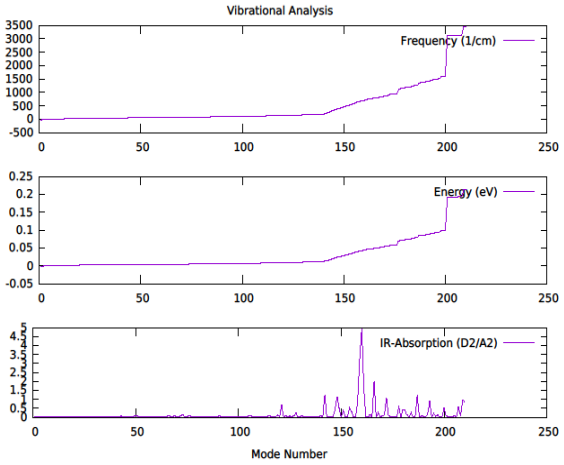

Figure 5: Frequency, free energy, and IR-absorption of an anthracene MJ

In Figure 5, a total of 210 vibrational modes was obtained. The first eight vibrational frequencies are negative, and it is a saddle point. The highest frequency of these vibrational modes is 3437.56 cm-1, corresponding to a free energy of 0.213 eV. Energy and frequency shift from 0.0997 eV and 1608.958 cm^{-1} to 0.1924 eV and 3103.627 cm-1 occur between 200 and 201 vibrational modes. The highest peak of IR absorption is 4.92 D2/Å2, which occurs at mode number 160, corresponding to a frequency of 688.52 cm-1 and an energy of 0.0427 eV. This result is similar to that of the Anthracene molecule, which has a maximum intensity of 1.83 D2Å-2 at mode 23, corresponding to the frequency of 715.47 cm^{-1} (Ibrahim *et al.,* 2024; Zongo *et al.,* 2021).

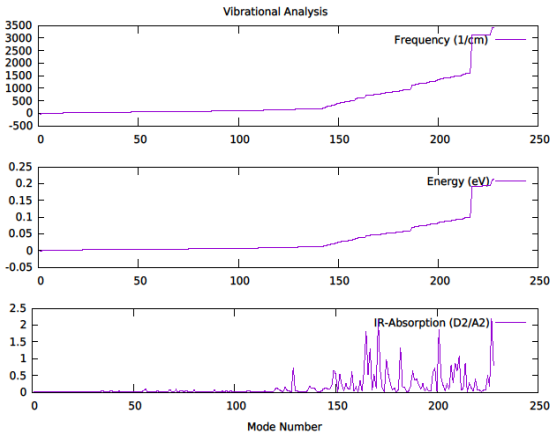

Figure 6: Frequency, free energy, and IR-absorption of tetracene MJ

Figure 6 shows vibrational frequency, free energy, and IR absorption as a function of vibrational mode for the tetracene MJ. It has 228 vibrational modes, with a maximum frequency of 3427.78 cm^{-1}, corresponding to a maximum energy of 0.2125 eV. There is a frequency and energy shift from 1610.31 cm-1 to 3101.46 cm-1 and from 0.0998 eV to 0.1923 eV, respectively. As for the IR absorption, there are at least three peaks present. At mode number 171, there is an IR-absorption peak value of 2.1433 $D^2Å^{-2}$, which corresponds to a 760.55 cm^{-1} frequency and 0.04715 eV energy. At mode number 201, the IR absorption is 1.8492 D2Å-2, corresponding to a frequency of 1353.82 cm-1 and an energy of 0.08393 eV. At mode number 227, the IR absorption is 2.1709 D2Å-2, corresponding to a frequency of 3411.82 cm-1 and an energy of 0.2115 eV. This implies that tetracene MJ is capable of photo-thermal conversion at the wavenumber 760.55 cm-1 (f equals 1.315×10 to the 0.55 cm^{-1} ($f = 1.315 \times 10^{-3} cm$).

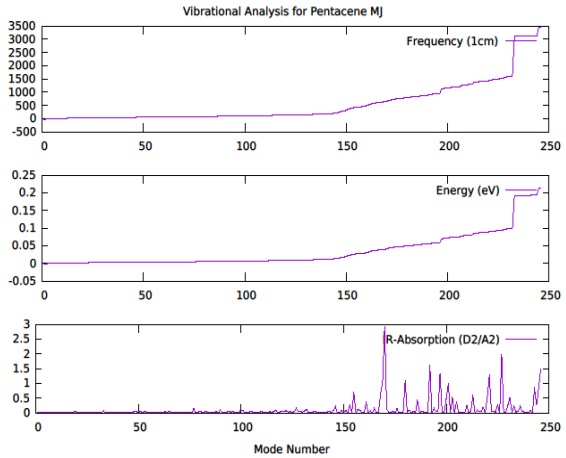

Figure 7: Frequency, free energy, and IR-absorption of a pentacene MJ

Figure 7: The first seven vibrational frequencies are negative, or saddle points. The highest frequency is 3454.01 cm^{-1}, corresponding to the highest energy of 0.214 eV. The frequency and energy shift from 1612.65 cm^{-1} and 0.0999 eV to 3103.01 cm^{-1} and 0.1924 eV, respectively. This occurs from mode number 232 to 233, respectively. The highest IR absorption is 2.93 D2/A2, occurring at mode number 170. This corresponds to the frequency of 648.71 cm^{-1} and energy of 0.0402 eV. These results imply that the pentacene MJ absorbed IR at a frequency (wavenumber) of 648.71 cm^{-1}. This is the upgrade to the pentacene molecule, which has a maximum absorption of 1.91 $D^2Å^{-2}$ (Kassim *et al.,* 2024).
The frequency (wavenumber) of the infrared radiation for the anthracene-, tetracene-, and pentacene-based molecular junctions is within the normal range of 4000 cm-1 to 600 cm-1, as suggested by Xin (2025).

Rotational and Translational Energies

Vibrational energies of rotation and translation for anthracene, tetracene, and pentacene MJs are presented in Tables 4, 5, and 6, respectively.

Science World Journal Vol. 21(No 1) 2026 https://dx.doi.org/10.4314/swj.v21i1.56
www.scienceworldjournal.org
ISSN: 1597-6343 (Online), ISSN: 2756-391X (Print)
Published by Faculty of Science, Kaduna State University

Table 4: Rotational and translational energies variations with temperature for anthracene MJ

Temperature [K]	Rotational free energy [eV]	Translational free energy [eV]
25.00000000	-0.04325246	-0.04104246
50.00000000	-0.09098472	-0.08955126
75.00000000	-0.14040787	-0.14087820
100.00000000	-0.19092907	-0.19403522
125.00000000	-0.24226678	-0.24855310
150.00000000	-0.29425516	-0.30415544
175.00000000	-0.34678466	-0.36065962
200.00000000	-0.39977737	-0.41793585
225.00000000	-0.45317509	-0.47588706
250.00000000	-0.50693260	-0.53443794
275.00000000	-0.56101380	-0.59352831
298.50000000	-0.61211884	-0.64952109
300.00000000	-0.61538919	-0.65310897
325.00000000	-0.67003417	-0.71313898
350.00000000	-0.72492798	-0.77358369
375.00000000	-0.78005281	-0.83441342
400.00000000	-0.83539323	-0.89560249

Table 5: Rotational and translational energies variations with temperature for tetracene MJ

Temperature [K]	Rotational free energy [eV]	Translational free energy [eV]
25.00000000	-0.04374187	-0.04106064
50.00000000	-0.09196356	-0.08958762
75.00000000	-0.14187611	-0.14093274
100.00000000	-0.19288673	-0.19410795
125.00000000	-0.24471385	-0.24864400
150.00000000	-0.29719166	-0.30426452
175.00000000	-0.35021057	-0.36078688
200.00000000	-0.40369270	-0.41808129
225.00000000	-0.45757983	-0.47605069
250.00000000	-0.51182676	-0.53461975
275.00000000	-0.56639738	-0.59372829
300.00000000	-0.62126217	-0.65332714
325.00000000	-0.67639657	-0.71337532
350.00000000	-0.73177980	-0.77383821
375.00000000	-0.78739404	-0.83468613
400.00000000	-0.84322387	-0.89589337

Table 6: Rotational and translational energies variations with temperature for pentacene MJ

temperature [K]	rotational free energy [eV]	translational free energy [eV]
25.00000000	-0.04397613	-0.04107872
50.00000000	-0.09243207	-0.08962378
75.00000000	-0.14257889	-0.14098697
100.00000000	-0.19382376	-0.19418026
125.00000000	-0.24588514	-0.24873439
150.00000000	-0.29859720	-0.30437299
175.00000000	-0.35185036	-0.36091343
200.00000000	-0.40556675	-0.41822592
225.00000000	-0.45968814	-0.47621339
250.00000000	-0.51416933	-0.53480053
275.00000000	-0.56897420	-0.59392716
300.00000000	-0.62407326	-0.65354408
325.00000000	-0.67944191	-0.71361034
350.00000000	-0.73505939	-0.77409131
375.00000000	-0.79090789	-0.83495731
400.00000000	-0.84697199	-0.89618263

From Tables 4, 5, and 6, it can be seen that both the translational and vibrational energies vary with environmental temperatures. These results obey the conservation of energy, since the total energy is conserved. The total energy content also varies with the size of the structure. This means that the more benzene rings in the structure, the higher its energy content.

Conclusion

In conclusion, the total energy, the maximum force, the number of Self_Consistency (SC) cycles, the number of relaxation steps, and the time taken to relax MJs depend on the molecular sizes. Thus, the anthracene MJ has the lowest energy, followed by the tetracene and pentacene MJs. The total number of basis functions does not depend on the molecular sizes.

The results showed that acene-based MJs absorb IR radiation much more than acene molecules. Thus, MJs are suitable candidates for photo-thermal or solar-thermal collection applications. Anthracene and pentacene MJs will be applicable for the medium frequency situations, while tetracene MJ is applicable for the much higher frequency situations.

REFERENCE

Babaji, G. (2015). SCF Cycle Convergence, Structure Optimization, and Vibrational Modes of Coumarin (α-Benzopyrone). *International Journal of Applied Physics and Mathematics,* 5(3), 206–217. DOI: 10.17706/ijapm.2015.5.3.206-217.

Blum, V., Gehrke, R., Hanke, F., Havu, P., Havu, V., Ren, X., & Reuter, M. S. (2009). Ab initio molecular simulations with numeric atom-centered orbitals. *Computer Physics Communications*, 2175–2196.

Donatella, B. & Lorentz, J. (2021). Comparison of Molecular Geometry Optimization Methods Based on Molecular Descriptors. *Mathematics*, 9, 2855. https://doi.org/10.3390/math9222855.

Engel, E. (2002). Orbital-dependent functional for the exchange-correlation energy. In Fiolhais, C., Nogueira, F., & Marques, M. (Eds), *A Primer in Density Functional Theory*. Springer, Berlin.

Galadanci, G.S.M., Ndikilar, C. E., Sabiu, S. A., Safana, A. (2015). Molecular Dynamics and Vibrational Analysis of Pentacene: RHF and DFT Study. *Chemistry and Materials Research,* 7(11), 16–23.

Heath, J. R., & Ratner, M. A. (2003). Molecular Electronics. *J. Physics Today,* AIP Publishing, **56**, (5), 43–49.

Ibrahim, K. L., Babaji G. & Nura, A. M. (2022). Charge Transport Enhancement in Anthracene Molecular Junction: Density Functional Theory Studies. *J. Mater. Sci. Res. Rev.,* vol. 10, no. 4, pp. 32–41, 2022; Article no.JMSRR.95693.

Ibrahim, K. L., Babaji, G. & Galadanci, G.S.M. (2024). Hybrid Molecular-Junction Technique for Enhancement of Electrical Conductance and Non-exponential Conductance-Length Dependence. *Sule Lamido Univ. J. of Sci. & Tech.,* 8 (1), 18–27. https://doi.org/10.56471/slujst.v7i.484.

Kassim L. I., Babaji, G., Galadanci G.S.M., Raymond, C. A., & Jamo, H. U. (2024). Energy Convergence in a Structure Optimization and Vibrational Modes of Some Acene Molecules. *DUJOPAS,* 10 (1c), 304-313. https://doi.org/10.4314/dujopas.v10i1c.30.

Kaneko, S., Motta, C,. Brivio G. P., & Kiguchi M. (2013). Mechanically Controllable Bi-stable States in a Highly Conductive Single Pyrazine Molecular Junction. *Nanotechnology,* 24, 315201.

Kohn, W., & Sham, L. J. (1965). Self-consistent equations including exchange and correlation effects. *Phys. Rev., 140*, A1133.

Lucas, D., Hyunhak, J., Nayan, K. P., Juan, S. G., & Joshua, H. (2021). Multidimensional Characterization of Single-Molecule Dynamics in a Plasmonic Nanocavity. *Angew. Chem. Int. Ed. 10.1002/anie. 202100886.* https://doi.org/10.1002/anie.202100886.

Preferencial, C. K., and John, D. T. (2018). First Principles Study of Electron Transport in Azulene Molecular Junction: Effect of Electrode Material on Electrical Rectification Behavior. *Journal of Computational Electronics*, 1-6.

Stegmann, T., Franco-Villafane, J. A., Ortiz, Y. P., Deffner, M., Herrman, C., Kuhl, U., … Seligman, T. H. (2020). Current vortices in aromatic carbon molecules. *Physical Review B*, 075405-1-10.

Xin, L. (2025). IR Spectrum and Characteristics: Absorption Bands. In Organic Chemistry I. *Kwantlen Polytechnic University,* pp. 6.1.1.

Yunus, A. C., & Afshin, J. G. (2015). Heat and Mass Transfer: Fundamentals and Applications. In Asia Higher Education, Engineering/Computer Science Mechanica. 5th Edition. *McGraw-Hill Education.* pp 153–234.

Zango, Z. U., Ramli, A., Jumbri, K., Sambudi, N. S., Isiyaka, H. A., AbuBakar, N. H. H. & Saad, B. (2021). Response surface methodology optimization and kinetics study for anthracene adsorption onto MIL-88(Fe) and NH_2-MIL-88(Fe) metal-organic frameworks. *IOP Conf. Series: Materials Science and Engineering.* **1092**, 012035.